(9) Magda, J. J.; Davis, H. T.; Tirrell, M. *J. Chem. Phys.* **1986**, *85*, 6674.
(10) Doi, M.; Yamamoto, I.; Kano, F. *J. Phys. Soc. Jpn.* **1984**, *53*, 3000.
(11) Maguire, J. F.; MacTague, J. P.; Rondelez, F. *Phys. Lett.* **1980**, *45*, 1891.
(12) Zero, K. M.; Pecora, R. *Macromolecules* **1982**, *15*, 87.
(13) Mori, Y.; Oocubo, N.; Hayakawa, R.; Wada, Y. *J. Polym. Sci., Polym. Phys. Ed.* **1982**, *20*, 2111.
(14) Odell, J. A.; Atkins, E. D. T.; Keller, A. *J. Polym. Sci., Polym. Lett. Ed.* **1983**, *21*, 289.
(15) Mori, Y.; Hayakawa, R. *Polym. Prepr. Jpn.* **1983**, *32*, 694.
(16) Russo, P. S.; Karasz, F. E.; Langley, K. H. *J. Chem. Phys.* **1984**, *80*, 5312.
(17) Keep, G. T.; Pecora, R. *Macromolecules* **1988**, *21*, 817.
(18) Fixman, M. *Phys. Rev. Lett.* **1985**, *54*, 337; **1985**, *55*, 2429.
(19) Bitsanis, I.; Davis, H. T.; Tirrell, M. *Macromolecules* **1988**, *21*, 2824.
(20) Onsager, L. *Ann. N.Y. Acad. Sci.* **1949**, *51*, 627.
(21) Doi, M.; Edwards, S. F. *Theory of Polymer Dynamics*; Clarendon Press: Oxford, 1986.
(22) Flory, P. J. *Proc. R. Soc. London, Ser. A* **1956**, *A234*, 73.
(23) Turk, P.; Lentelme, F.; Friedman, H. *J. Chem. Phys.* **1977**, *66*, 3039.
(24) Van Gunsteren, W. F.; Berendsen, H. J. C. *Mol. Phys.* **1982**, *45*, 637.
(25) Chandrasekhar, S. *Rev. Mod. Phys.* **1943**, *15*, 1.
(26) Van Kampen, N. G. *Stochastic Processes in Physics and Astronomy*; North Holland: Amsterdam, 1981.
(27) Gardiner, C. W. *Handbook of Stochastic Methods for Physics, Chemistry and Natural Sciences*; Springer-Verlag: Berlin-Heidelberg, 1983.
(28) Ceperley, D.; Kalos, M. H.; Lebowitz, J. L. *Macromolecules* **1981**, *14*, 1472.
(29) Metropolis, N.; Rosenbluth, A. W.; Rosenbluth, M. N.; Teller, A. H.; Teller, E. *J. Chem. Phys.* **1953**, *21*, 1087.
(30) Rossky, P. J.; Doll, J. D.; Friedman, H. L. *J. Chem. Phys.* **1978**, *69*, 4268.
(31) Rao, M.; Pangali, C.; Berne, B. J. *Mol. Phys.* **1979**, *37*, 1773.
(32) Rao, M.; Berne, B. J. *J. Chem. Phys.* **1979**, *71*, 129.
(33) Verlet, L. *Phys. Rev.* **1967**, *159*, 98.
(34) Lebowitz, J. L.; Rubin, E. *Phys. Rev.* **1963**, *131*, 2381.
(35) Resibois, P.; Davis, H. T. *Physica* **1964**, *30*, 1077.
(36) Wada, A.; Kihara, H. *Polym. J.* **1972**, *3*, 482.
(37) Tsuji, K.; Ohe, H.; Watanabe, H. *Polym. J.* **1973**, *4*, 553.

Dynamic Behavior of Θ Solutions of Polystyrene Investigated by Dynamic Light Scattering

Taco Nicolai, Wyn Brown,* and Robert M. Johnsen

Institute of Physical Chemistry, University of Uppsala, 751 21 Uppsala, Sweden

Petr Stěpánek

Institute of Macromolecular Chemistry, Czechoslovak Academy of Sciences, 162 06 Prague 6, Czechoslovakia. *Received June 2, 1989; Revised Manuscript Received August 9, 1989*

ABSTRACT: Relaxation time distributions from dynamic light scattering (DLS) (obtained from the correlation curves using a Laplace inversion routine REPES), typically covering about 8 decades in relaxation time, have been determined for solutions of polystyrene in cyclohexane at 35 °C (Θ conditions) over a wide span of polymer concentrations from very dilute to far into the semidilute regime. The relaxation time distributions increase in complexity with increasing polymer concentration. The results from the semidilute solutions are compared to a theory developed by Brochard and de Gennes and are shown to agree only partially. The results indicate that DLS is a possible tool for the investigation of viscoelastic properties of semidilute polymer solutions.

Introduction

The scaling description of semidilute polymer solutions[1-3] has been a major inspiration of new ideas in the physics of static and dynamic properties of polymers in solution. It has led to predictions whose experimental verification required precisely the space and time resolution offered by light scattering and neutron scattering. A broad review that includes the application of dynamic light scattering (DLS) to this problem area is provided by ref 4.

A central prediction of the scaling theory for semidilute solutions in thermodynamically good solvents is that a single characteristic length exists in such systems and consequently only one dynamic process should be observed, characterized by a cooperative diffusion coefficient (D). Experimentally, it has been found, however, that although cooperative diffusion dominates in semidilute solutions in good solvents, other processes participate and give rise to deviations from a single exponential decay of the autocorrelation function of the scattered light. This effect, typified by low-frequency modes in the decay spectrum, becomes very pronounced with a decrease in solvent quality toward Θ conditions.[5-15]

Brochard and de Gennes[16,17] have developed scaling expressions for Θ systems. They propose two limiting regimes: at small scattering vectors (q) (such that $Dq^2 < T_r^{-1}$, where T_r is the characteristic disentanglement time for the chains or the terminal time from viscoelastic measurements) the restoring force for the concentration fluctuations, originating from the osmotic compressibility, leads to a cooperative diffusion coefficient that is linearly proportional to the polymer concentration. At scattering vectors (corresponding to $Dq^2 > T_r^{-1}$), they predict that the correlation function is bimodal. The fast mode characterizes the cooperative diffusion and the other mode, which is independent of the scattering vector, char-

0024-9297/90/2223-1165$02.50/0

acterizes the structural relaxation of the transient network.

Adam and Delsanti[9] analyzed the correlation function at large scattering vectors in terms of two modes as had been predicted by Brochard and de Gennes: the fastest mode was found to be diffusive and the slowest was independent of the scattering vector and close to the longest relaxation time obtained by viscoelastic measurements.

Others[10-15] have subsequently shown that (in various Θ systems) the decay time spectrum is even more complicated. Besides the diffusive mode they observed a number of slower modes that were independent of the scattering vector. The slowest of these modes was of the order T_r.

Here we report results from DLS experiments on Θ solutions of polystyrene over a broad range of polymer concentrations from very dilute to far into the semidilute regime. It will be shown that the autocorrelation function of the scattered light gradually changes when we increase the concentration from a relatively simple situation for dilute systems, where we measure the diffusion of individual chains, to a complex situation for semidilute systems, where we measure a fast diffusive mode and a whole range of slower modes. We will interpret the diffusive mode in terms of the theory given by Brochard and de Gennes and extended by Adam and Delsanti. The slower modes can probably be related to the viscoelastic properties, which are also measured in mechanical measurements, but not in the simple way given by Brochard and de Gennes.

Theory

If the influence of the solvent is ignored, the intensity fluctuations of light scattered from dilute solutions of monodisperse linear polymers result from translational diffusion of the polymer chains and intramolecular motions. The latter become important when $qR_g > 1$ where R_g is the radius of gyration of the coils and q is the scattering wave vector light given by $q = (4\pi n/\lambda) \sin(\theta/2)$ with n the refractive index, λ the wavelength, and θ the scattering angle. By use of the Rouse–Zimm model for polymers the intramolecular motions can be described in terms of a series of internal modes.[3,18,19] Writing only the first internal mode explicitly, the field autocorrelation function of the scattered light normalized by the average intensity is given by[20]

$$g(t) = \frac{\langle E(0)E(t)^* \rangle}{\langle I \rangle} = A_1 e^{-\Gamma_1 t}(1 + A_2 e^{-\Gamma_2 t} + ...) \quad (1)$$

where $\Gamma_1 = Dq^2$ with D the translational diffusion coefficient of the coils and $\Gamma_2 = 2/\tau_1$ with τ_1 the relaxation time of the first internal mode. The relative amplitudes of the internal modes are strongly dependent on the scattering vector but their relaxation times are q independent. At infinite dilution the diffusion coefficient is related to the hydrodynamic radius of the coils (R_h) through the Stokes–Einstein relation

$$D^0 = \frac{kT}{6\pi\eta_s R_h} \quad (2)$$

with η_s the solvent viscosity, k the Boltzmann constant, and T the absolute temperature.

For Θ solvents D decreases with increasing concentration due to friction between the chains since the second virial coefficient is zero.[21]

When the concentration increases over a certain value (C^*) the coils overlap and multichain interactions become important. Solutions in which the coils overlap strongly but the segment friction still depends only on the solvent viscosity are called "semidilute". The only attempt to describe the component modes contributing to light scattered from semidilute solutions of linear polymers at Θ conditions was made by Brochard and de Gennes.[16,17] In their theory (which we briefly summarize below) the spontaneous concentration fluctuations are described as weak sinusoidal modulations of the average concentration (C):

$$\delta C(x,t) = \delta C \cos(qx) e^{-t/\tau_q} \quad (3)$$

with τ_q the relaxation time of the modulation of the wave vector q with which we probe in a DLS experiment. The response to these concentration fluctuations is written as a balance between a restoring force in terms of the longitudinal elastic modulus (M) on the one hand and the friction between the chains and the solvent on the other:

$$\frac{C}{\mu}\frac{\delta u}{\delta t} = M\nabla^2 u \quad (4)$$

where u is the displacement of the chains and μ is the effective mobility. In a semidilute Θ solution the chains are always entangled and are thought to form a transient network. Therefore M may be split into an osmotic modulus E_o due to thermodynamic interactions and a gel modulus (E_g) due to the entanglements.

The osmotic modulus is related to the osmotic pressure (π):

$$E_0 = C(\delta\pi/\delta C) \quad (5)$$

Under Θ conditions excluded-volume effects due to the binary interactions between chain segments are absent, which means that the osmotic modulus is due mainly to ternary interactions and thus $E_o \sim C^3$ where it is assumed that the segment distribution of the polymers is Gaussian.

The gel modulus is related to the density of entanglements that are due to topological interactions between two chains and therefore $E_g \sim C^2$. One has to take into account, however, that the entanglements have a finite lifetime, which depends strongly on the polymer concentration and the molecular weight. As a consequence, the gel modulus depends on the frequency (ω) of the concentration fluctuations and thus the wave vector q at which we probe these fluctuations. If one assumes a single characteristic time (τ_r) in which the chains disentangle, the elastic force of the transient gel may be modeled by a single dashpot and spring in series and M becomes

$$M(\omega) = E_o + E_g \frac{i\omega\tau_r}{1 + i\omega r\tau_r} \quad (6)$$

For very low frequencies the polymers will have time to disentangle and the concentration fluctuations relax as in a viscous solvent with a characteristic relaxation time determined by the osmotic modulus only

$$\tau_q^{-1} = \frac{\mu}{C}E_0 q^2 = D_h q^2 \quad (7)$$

Here D_h is the cooperative diffusion coefficient in this so-called hydrodynamic regime defined by

$$D_h = kT/6\pi\eta_s\xi_h \quad (8)$$

where the hydrodynamic correlation length ξ_h is expected to be inversely proportional to the polymer concentration for Θ solvents and independent of the molecular weight.

For very high frequencies, on the other hand, the entan-

glements may be considered to be "frozen" and the concentration fluctuations relax as in a permanent gel with a characteristic relaxation time determined by both the osmotic modulus and the gel modulus. For this case we may write

$$\tau_q^{-1} = \frac{\mu}{C}(E_0 + E_g)q^2 = D_g q^2 \tag{9}$$

Here $D_g = D_h + D_g^0$ is the cooperative diffusion coefficient in this so-called gel regime with D_h given by eq 8 and

$$D_g^0 = \frac{\mu}{C}E_g = f\frac{kT}{6\pi\eta_s a} \tag{10}$$

where a is the size of a monomer and f is a numerical coefficient depending on the efficiency with which entanglements are formed. D_g^0 is independent both of the concentration and of the molecular weight.

The normalized autocorrelation function of the scattered light ($g_{(1)}(t)$) has been derived by Brochard and de Gennes with the assumption that $E_g \gg E_0$. Later a modification was given by Adam and Delsanti[9] to cover the case of $E_g \geq E_0$. Assuming that $D_g > D_h$, $g_{(1)}(t)$ may be written as a sum of two exponentials:

$$g_{(1)}(t) = A_f e^{-t/\tau_f} + A_s e^{t/\tau_s} \tag{11}$$

The amplitudes of the fast (f) and the slow (s) modes are given by

$$A_f = \frac{\tau_f - T_r}{\tau_s - \tau_f} \qquad A_s = \frac{\tau_s - T_r}{\tau_s - \tau_f} \tag{12}$$

For $D_g q^2 \ll T_r^{-1}$, i.e., in the hydrodynamic regime, the fast and slow relaxation times are $\tau_f = T_r$ and $\tau_s = (D_h q^2)^{-1}$. The amplitude of the fast mode, however, becomes very small in comparison to the slow mode so that the autocorrelation function is characterized by a single, angle-dependent, relaxation time.

For $D_g q^2 \gg T_r^{-1}$, i.e., in the gel regime, the fast and slow relaxation times are

$$\tau_f = 1/(D_g)q^2 \qquad \tau_s = T_r(D_g/D_h) \tag{13}$$

In this limit the ratio of the amplitudes of the fast and the slow modes becomes

$$\frac{A_f}{A_s} = \frac{1}{D_g/D_h - 1} = \frac{D_h}{D_g^0} \tag{14}$$

Inserting the expressions for D_h and D_g^0 given in eq 8 and 10 into eq 14, we obtain the following expression for D_g

$$\frac{6\pi\eta_s}{kT}D_g = \frac{1}{\xi_h} + \frac{f}{a} \tag{15}$$

In the foregoing discussion it has been assumed that $q\xi_h \ll 1$, i.e., we have not considered internal modes of parts of the chains that are correlated. If q^{-1} is smaller than the correlation length but is still larger than the distance between entanglements, the first relaxation time is expected to be no longer linearly proportional to q^2. D_g calculated as $1/(\tau_f q^2)$ decreases in this case with increasing q. For even larger wave vectors internal modes of parts of the chains between entanglements are probed, which are expected to be the same as for a single chain with the length of these parts.

Experimental Section

Polystyrene solutions were prepared using polymers from Toya Soda Ltd. Japan: $M_w = 3.8 \times 10^6$, $M_w/M_n = 1.05$, $M_w = 5.48 \times 10^6$, $M_w/M_n = 1.05$, $M_w = 1.28 \times 10^6$, $M_w/M_n = 1.05$. The solvent was spectroscopic grade cyclohexane from Merck, Darmstadt, FRG, and was used without further purification except for drying over 3-Å molecular sieves. The solutions were made by initial dissolution of the polymer in cyclopentane followed by centrifugation. The upper portion was used and the cyclopentane evaporated and replaced by a measured amount of filtered cyclohexane in the measuring cell, which was then flame-sealed. The solutions were allowed to mature for months prior to use.

The experimental arrangement has been described previously.[10] The light source was either a 488-nm Ar ion laser or a 632-nm He–Ne laser. An ALV-Langen Co., multibit, multi-τ autocorrelator was operated with 23 simultaneous sampling times (covering, for example, delay times in the range 1 μs to 1 min) in the logarithmic mode and 191 channels. The stability of the photon count at all angles indicated that the solutions were essentially dustfree.

Method of Analysis. For the analysis of the measured autocorrelation curve, an inverse Laplace transformation ($g(t) = \int_0^\infty A(\tau)e^{-t/\tau}\,d\tau$) was performed using a constrained regularization calculation program called REPES[22] to obtain the distribution $A(\tau)$ of relaxation times. The algorithm differs in a major respect from CONTIN developed by Provencher[23] in that the relevant computer program directly minimizes the sum of the squared differences between the experimental and calculated $g_{(2)}(t)$ functions ($g_{(2)}(t) = g_{(1)}^2(t)$), modified by a penalizing term. We have compared analyses using REPES with those using CONTIN and MAXENT,[24,25] which are other calculation routines used to perform the Laplace transformation using a different minimization procedure, for a number of correlation curves. The results were found to be quite similar when the same degree of smoothing was used. REPES, however, is much faster than the current implementations of CONTIN and MAXENT on personal computers. The range of relaxation times allowed in the fitting was usually between 10 μs and 100 s with a density of 12 points per decade. In Figure 1 an example is given of a correlation curve together with the result of the analysis using REPES and the residuals to the fit. The relaxation rates are obtained from the moments of the peaks of the relaxation time distribution or, when the peaks were partly overlapping, from the peak positions.

CONTIN yields broad distributions with multiple peaks in the relaxation spectrum in its unsmoothed analysis. The same is true for REPES and it is therefore necessary to use smoothing in the analysis. The influence of the use of different degrees of smoothing in the analysis is shown in Figure 2. The degree of smoothing is changed by selecting a value for the "probability to reject" (P) identical with that used in CONTIN; the higher P is the greater the smoothing. It is clear that for this example the number of peaks is independent of the degree of smoothing from low smoothing to high smoothing, indicating that the analysis does not give spurious peak multiplicity due to the amount of noise in the data. Smoothing corresponding to a P value of 0.5 was chosen as standard in all our analyses. This degree of smoothing corresponds to the default value of the so-called "chosen" solution in CONTIN. An additional check on the possible occurrence of spurious peaks may be obtained by analysis of a simulated correlation function consisting of a continuous broad distribution of relaxation times with noise equal to the residuals resulting from an analysis of the experimental correlation curve. In this case we found that REPES yields the broad distribution even when low smoothing is used; see Figure 3. However, it cannot be excluded that a small systematic bias in the experimental data, which does not show up in the residuals, influences the resolution of the relaxation time distributions.

It has been shown in simulations that a spike added to a broad distribution of relaxation times may cause an artificial split up of the broad distribution into discrete peaks.[26] Therefore we have subtracted the relatively sharp fast mode from the experimental correlation curve and reanalyzed the data. It turns out that the values of the slower modes are not significantly different in the absence of the faster mode.

It has been found that in order to obtain a stable detailed relaxation time spectrum as exemplified in Figure 2, it is necessary that the noise level on the experimental correlation func-

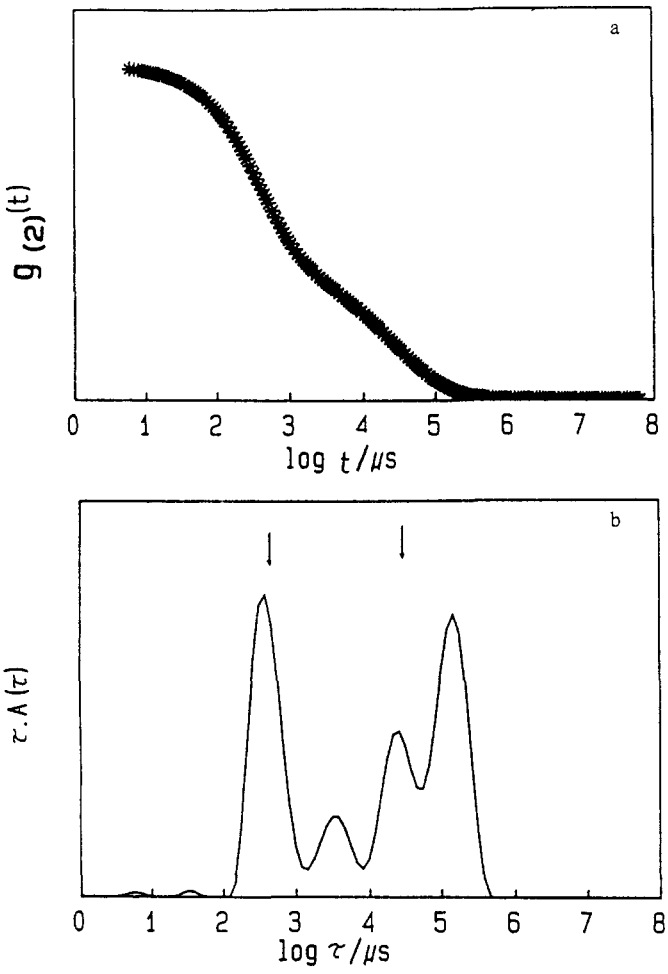

Figure 1. Experimental correlation function (a) with its relaxation time distribution (b) obtained from REPES of polystyrene in cyclohexane at 35 °C (M_w = 3.8 × 10^6, C = 6.4 × 10^{-2} g mL^{-1}, q^2 = 2.0 × 10^{14} m^{-2}). The residuals are shown in part c. The results of a forced fit to a bimodal function are indicated with arrows in (b) and the residuals of this fit are shown in part d.

tion is very low. The data were collected over time periods between 3 and 15 h leading to typical base-line values of the order of magnitude of 10^{15}.[39] Relaxation time spectra obtained from measurements on solutions of polystyrene in different Θ solvents reported earlier[12,13] show much less detail due to the higher noise level on the correlation curves.

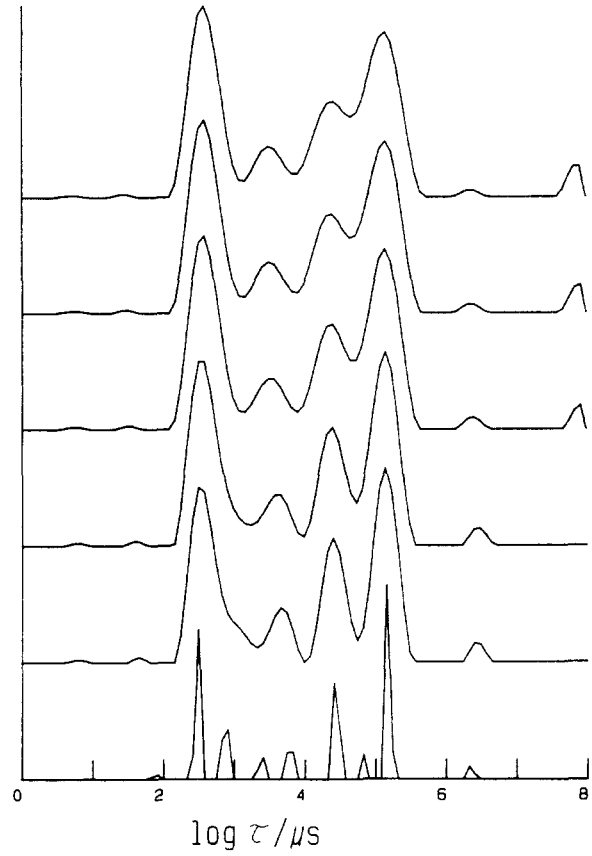

Figure 2. Relaxation time distributions obtained from REPES for different degrees of smoothing. From bottom to top P is 0.00, 0.01, 0.1, 0.9, 0.99, and 0.999. System as in Figure 1.

The necessity of using a Laplace inversion in the analyses in this case becomes clear when we try to analyze the experimental autocorrelation functions in terms of a double-exponential function. Force fitting to a double exponential plus the floating base line leads to very poor results as is clear from the residuals shown in Figure 1d. The two relaxation times that were found are indicated in Figure 1b. It follows that a double-exponential function is an oversimplified representation of the experimental autocorrelation curve and that an analysis via a Laplace transformation is the only realistic method to treat data in this case.[40]

Results and Discussion

DLS experiments have been performed on solutions of polystyrene with a molecular weight M_w = 3.8 × 10^6 over a wide range of concentrations from very dilute (8 × 10^{-4} g/mL) to far in the semidilute regime (1.3 × 10^{-1} g/mL). Also polystyrene samples with three different molecular weights (1.28 × 10^6, 3.8 × 10^6, 5.48 × 10^6) have been measured at a fixed concentration (~6.5 × 10^{-2} g/mL). The concentration C^* separating the dilute from the semidilute regime is taken here as the concentration where the chains start to overlap:

$$C^* = 3M/4\pi R_g^3 N_A \qquad (16)$$

where N_A is Avogadro's number. In the calculation of C^* we have used a well-corroborated relationship between the molecular weight and the radius of gyration under Θ conditions from the literature ($R_g = 0.29M_w^{0.5}$). For the systems investigated here C^* becomes 1.4 × 10^{-2}, 8 × 10^{-3}, and 6.6 × 10^{-3} g/mL for M_w equal to 1.28 × 10^6, 3.8 × 10^6, and 5.48 × 10^6, respectively. From the measured correlation functions, relaxation time distribu-

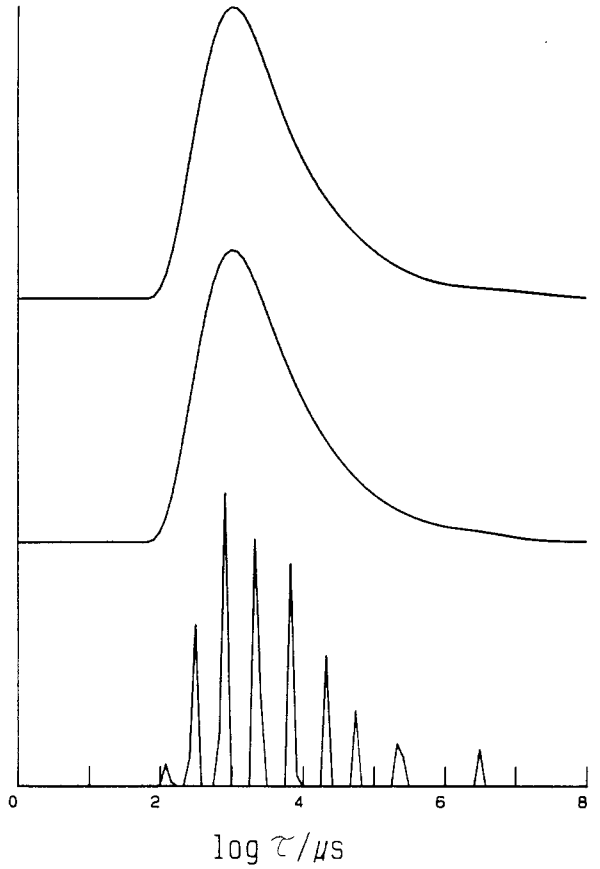

Figure 3. Relaxation time distributions obtained from REPES for different degrees of smoothing, of a simulated broad Pearson distribution with added noise as shown in Figure 1c. From bottom to top P is 0.00, 0.01, and 0.1.

tions were obtained as described above. We will first discuss the measurements performed at concentrations far below C^*, then the measurements performed at concentrations much larger than C^*, and finally those at concentrations around C^*.

Dilute Solutions. Relaxation time distributions obtained from a dilute solution ($C = 8 \times 10^{-4}$ g/mL) at several different scattering vectors are shown in Figure 4. At low values of the scattering vector we obtain a single narrow peak implying that the correlation function is essentially single exponential. Plotting the relaxation rate ($\Gamma = 1/\tau$) as a function of q^2, we observe a linear dependence (see Figure 5), and an effective diffusion coefficient D_e has been calculated by a linear least-square fit to the data. The value of the D_e is given in Table I and compares well with literature values of the diffusion coefficient at infinite dilution.

For values of the scattering vector where $qR_g \geq 1$, we expect to see contributions from intramolecular motions (see eq 1). This is the reason for the appearance in Figure 4 of the small peak at the fast end of the relaxation time distributions. These intramolecular motions have been the subject of an earlier investigation,[27] and we will only mention here that the position of the small peak on the time axis is close to that expected theoretically. The theoretical values for the relaxation time of the first internal mode are indicated in the figures. In the calculation Zimm's non-free-draining model was assumed as this model gives the best agreement with the experimental data.

Increasing the polymer concentration slightly (up to 5×10^{-3}) we observe no major changes. The value for the diffusion coefficient decreases as expected with increasing polymer concentration (see Table I) due to an increasing friction between the chains.

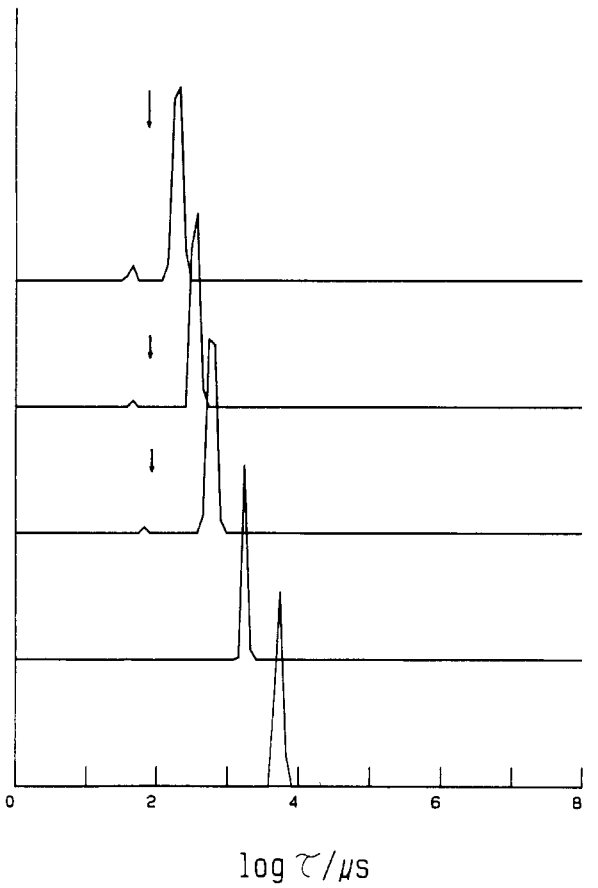

Figure 4. Relaxation time distributions obtained from REPES for a dilute solution of polystyrene in cyclohexane at 35 °C ($M_w = 3.8 \times 10^6$, $C = 0.8 \times 10^{-3}$ g mL^{-1}) for different scattering vectors. From bottom to top $q^2 = 0.24 \times 10^{14}$, 0.93×10^{14}, 2.0×10^{14}, 4.0×10^{14}, and 7.0×10^{14} m^{-2}. The arrows indicate the theoretical positions of the first internal mode.

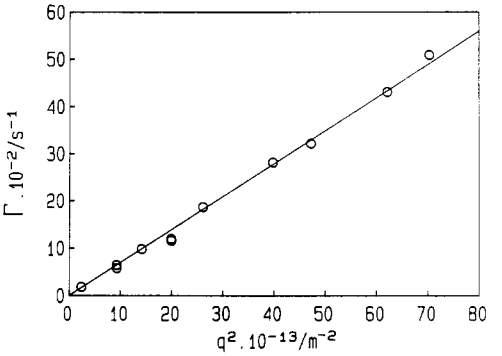

Figure 5. Plot of the decay rates of the dominant slow mode versus q^2 for a dilute solution of polystyrene in cyclohexane at 35 °C. System as in Figure 4.

Semidilute Solutions. Turning our attention to the other end of the investigated concentration range, we will now look at the results from solutions in the concentration range 3.7×10^{-2}–12.6×10^{-2} g/mL, which may be considered to be well in the semidilute regime. For these concentrations the contribution of internal modes to the correlation function is negligible in the range of scattering vectors used.

Figure 6 shows relaxation time distributions for several different scattering vectors, where the polymer concentration of the measured solution was 6.4×10^{-2} g/mL and $M_w = 3.8 \times 10^6$. The distributions show great complexity with relaxation times over a broad (several decades) time range. This complexity has been observed before for other semidilute solutions under Θ conditions,

Table I
Experimental Values of the Effective Diffusion Coefficient at Different Polymer Concentrations for Polystyrene in Cyclohexane at 35 °C[a]

$10^{-2}C/(\text{g mL}^{-1})$	$10^{12}D_e/(\text{m}^2\ \text{s}^{-1})$
0.08	6.9
0.2	6.7
0.52	4.6
0.8	3.9
3.7	10.6
6.4	14.8
6.6 ($M_w = 5.48 \times 10^6$)	13.8
6.6 ($M_w = 1.28 \times 10^6$)	13.3
10.2	17.9
12.6	21.1

[a] $M_w = 3.8 \times 10^6$ or as otherwise indicated in the table.

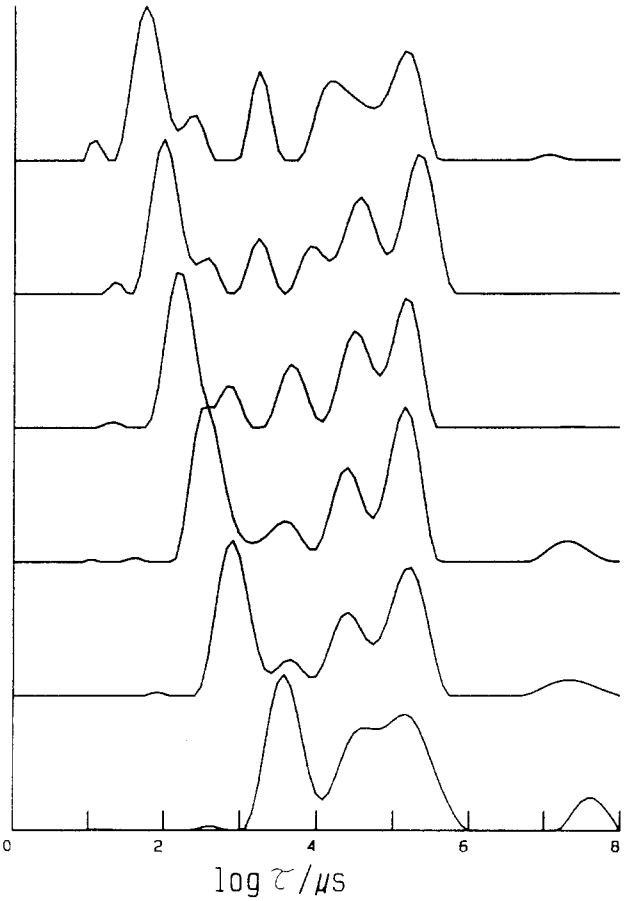

Figure 6. Relaxation time distributions obtained from REPES for a semidilute solution of polystyrene in cyclohexane at 35 °C ($M_w = 3.8 \times 10^6$, $C = 6.4 \times 10^{-2}$ g mL^{-1}) for different scattering vectors. From bottom to top $q^2 = 0.24 \times 10^{14}$, 0.93×10^{14}, 2.0×10^{14}, 4.0×10^{14}, 7.0×10^{14}, and 11.8×10^{14} m^{-2}.

although with much lower resolution.[12,15] Inspection of the distributions reveals that the value of one (fast) relaxation time strongly decreases with an increasing value of the scattering vector. The other (slower) modes seem to be at most only weakly dependent on the value of the scattering vector. In figure 7 the relaxation times of the major peaks at the extremes of the relaxation distributions are plotted as a function of q^2. It is clear that the fast mode is diffusive and that the slowest mode is essentially independent of the scattering vector. As the fast mode moves with increasing scattering vector to shorter times, more intermediate modes are observed, all of which depend only weakly on the scattering vector. A very similar picture is obtained for the other concentrations and molecular weights: one fast diffusive mode and a number of largely q-independent modes that stretch out on the time axis from the diffusive mode to the slowest mode, which is independent of the scattering angle. The lowest molecular weight sample behaves differently at small scattering vectors, however, a feature which we will discuss below. Figure 8 shows the relaxation time distributions at the same scattering vector for four different polymer concentrations at a fixed molecular weight and three different molecular weights at a fixed concentration. When the polymer concentration is increased at a fixed molecular weight it is apparent that (1) the diffusive mode

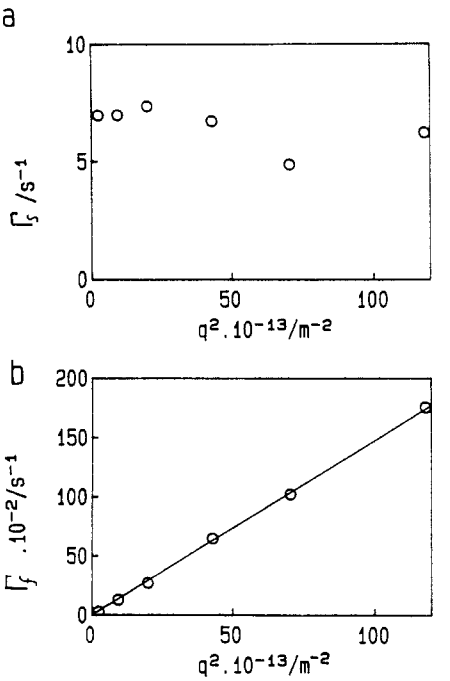

Figure 7. Plot of the decay rates of the slowest (a) and the fastest (b) mode versus q^2, for a semidilute solution of polystyrene in cyclohexane at 35 °C. System as in Figure 6.

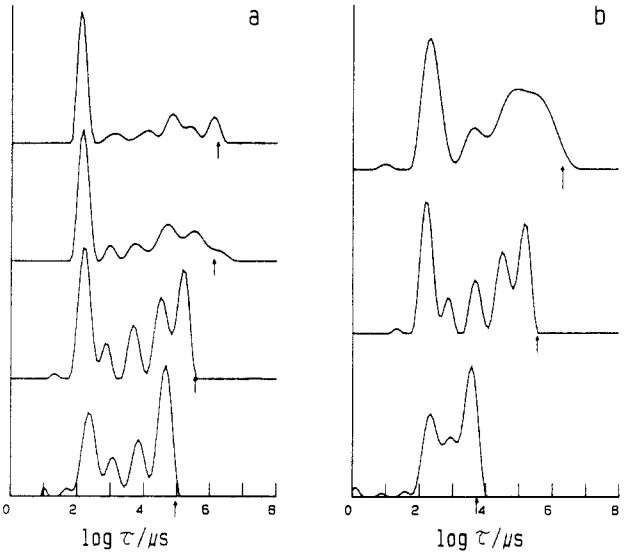

Figure 8. Relaxation time distributions obtained from REPES for semidilute solutions of polystyrene in cyclohexane at 35 °C. Part a shows the results for different polymer concentrations at a fixed molecular weight and scattering vector ($M_w = 3.8 \times 10^6$, $q^2 = 4.0 \times 10^{14}$ m^{-2}): C is 3.7×10^{-2}, 6.4×10^{-2}, 10.2×10^{-2}, and 12.6×10^{-2} g mL^{-1} (bottom to top). Part b shows the results for different molecular weights at a fixed concentration and scattering vector ($\sim 6.5 \times 10^{-2}$ g mL^{-1}, $q^2 = 4.0 \times 10^{14}$ m^{-2}): M_w is 1.28×10^6, 3.8×10^6, and 5.48×10^6 (bottom to top). Values of $T_r(D_g/D_h)$ are indicated by arrows.

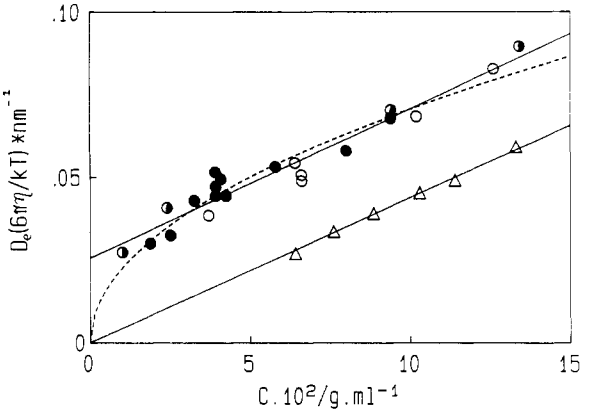

Figure 9. Plot of $D_e(6\pi\eta_s/kT)$ obtained from DLS (open circles) and classical gradient (triangles) measurements versus the polymer concentration (C). Data from ref 9 (filled circles) and ref 13 (half-filled circles) are also shown. The broken line represents a nonlinear least-squares fit to $y = aC^x$, and the straight lines are linear least-squares fits to $y = aC + b$.

becomes faster, (2) the value of the slowest relaxation time increases, (3) the relative amplitude of the diffusive mode increases, and (4) the relative amplitudes of the slower modes change with respect to each other.

When increasing the molecular weight at a fixed concentration we find that (1) the diffusive mode and its relative amplitude do not change significantly and (2) the relaxation time of the slowest mode increases strongly.

An immediate conclusion from these observation is that the theory of Brochard and de Gennes discussed above explains only some of the essential features of the experimental findings. In comparing the observations in more detail with the theory, we will first concentrate on the diffusive mode and thereafter look at the slower modes.

From eq 15 it is expected that the experimentally obtained diffusion coefficient (D_e) multiplied by a factor $6\pi\eta_s/kT$ is the sum of ξ_h^{-1} and f/a, where it is assumed that we are in the gel regime as the characteristic disentanglement time of the chains is much slower than $(Dq^2)^{-1}$ for all DLS measurements on semidilute solutions reported here, with one, already mentioned, exception.

Values of $D_e(6\pi\eta_s/kT)$ are plotted as a function of the polymer concentration in Figure 9 (upper line) together with two sets of data obtained from the literature.[9,13] All data have been corrected for backflow by division by $(1 - \varphi)$ where φ is the volume fraction of the polymer.[28] Other experimental data found in the literature[5-7] deviate systematically and are not included in Figure 9. The data, which cover a range of molecular weights between 1.3×10^6 and 20×10^6, show that the diffusion coefficient does not depend significantly on the molecular weight, in agreement with the theoretical expectations. A linear least-square fit through the data seems appropriate and gives

$$(6\pi\eta_s/kT)D_e = 4.5 \times 10^6 C + 2.6 \times 10^5 \text{ cm}^{-1} \quad (17)$$

With the present spread, the data can also be expressed by a simple scaling relation over the limited range of concentrations in the semidilute regime. The dashed curve drawn through the data in Figure 9 is found by a least-square fitting as $2.3 \times 10^6 C^{0.5}$ cm^{-1}. Lacking theoretical support, however, expression as a scaling relationship appears to be misleading.

If we assume that eq 15 correctly describes the observed diffusion coefficient, we obtain $\xi_h = 2.2 \times 10^{-7} C^{-1}$ cm and $a/f = 38$ nm. Taking for the monomer size $a = 0.75$ nm, we obtain $f = 2.0 \times 10^{-2}$, which is somewhat greater than the value found for polystyrene melts (5.6×10^{-3}).[29] The difference is, however, small enough for the assumption that f is constant over the concentration range investigated.

Independent values for ξ_h may be obtained from classical gradient measurements. With this technique the diffusion coefficient is obtained by measuring macroscopic displacements of the coils. Therefore entanglements are not important and the measured diffusion coefficient is given by eq 8. Values taken from Roots and Nyström[30] are also shown in Figure 9 (lower line). A linear least-square fit through the data yields $\xi_h = 2.3 \times 10^{-7} C^{-1}$ cm, which is nearly identical with the result from DLS experiments.

From these results we may conclude that the diffusive mode is well described by eq 15, which means that the cooperative diffusion coefficient is due to a combination of the elastic forces of the transient gel and ternary thermodynamic interactions.

According to the theory discussed above one would expect to observe, as well as a diffusive mode, a single q-independent relaxation mode. This is a consequence of the fact that the frequency dependence of the gel modulus is modeled as a single Maxwell element. Mechanical measurements have shown, however, that this model is an oversimplification and does not correctly describe the viscoelastic behavior of linear polymers.[31] In order to explain the viscoelastic behavior, other faster relaxation modes have to be invoked besides a slowest mode connected with the characteristic disentanglement time of the whole transient network. A more realistic model for the frequency dependence of the gel modulus is needed to establish whether the observed distribution of q-independent relaxation times reflects the viscoelastic properties of the transient network. The use of two parallel Maxwell elements as a model, for example, would lead to three relaxation times characterizing the autocorrelation function. Calculation of the relaxation times and amplitudes is cumbersome, however, and, in view of the fact that three relaxation modes are not enough to describe the experimental autocorrelation curve, inadequate. Wang and Fisher[32] recently developed a theory to relate, in the case of polymer melts, the autocorrelation curve measured in DLS to the longitudinal compliance ($D(t)$), which in turn is related to the longitudinal elastic modulus. Comparison between DLS and mechanical measurements shows a satisfactory agreement with this theory.[33] If $D(t)$ is available a similar relation could perhaps also be used in the case of semidilute solutions in order to obtain a more realistic comparison between DLS and mechanical measurements.

Unfortunately only few mechanical experiments have been performed on semidilute polymer solutions.[34-38] In all cases the shear elastic modulus ($G(t)$) has been measured. In DLS the longitudinal elastic modulus is probed so that in order to make a comparison we have to assume that $G(t)$ is simply proportional to $M(t)$. The slowest ("terminal") relaxation time observed in these measurements was found to increase with increasing concentration and increasing molecular weight as is observed for the slowest relaxation time obtained from DLS. Adam and Delsanti[35] measured the shear modulus for polystyrene in cyclohexane at 35 °C and determined the terminal relaxation time as a function of the molecular weight and the concentration. These data may be directly compared with DLS measurements reported here. If the transient gel is modeled as a single Maxwell element, the relationship between the slowest (terminal) relaxation time measured in mechanical experiments and the slowest relax-

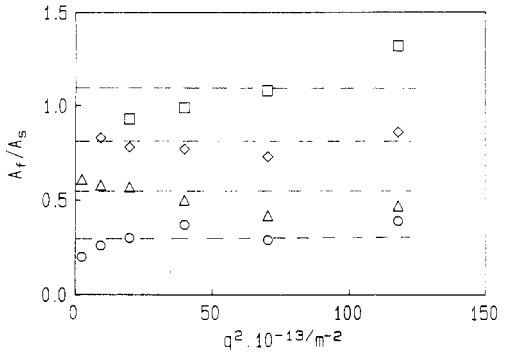

Figure 10. Values of A_f/A_s versus q^2 for different concentrations of polystyrene in cyclohexane at 35 °C ($M_w = 3.8 \times 10^6$). The concentrations are 3.7×10^{-2} (circles), 6.4×10^{-2} (triangles), 10.2×10^{-2} (diamonds), and 12.6×10^{-2} g mL^{-1} (squares). The straight lines are drawn through the average values plotted in Figure 11.

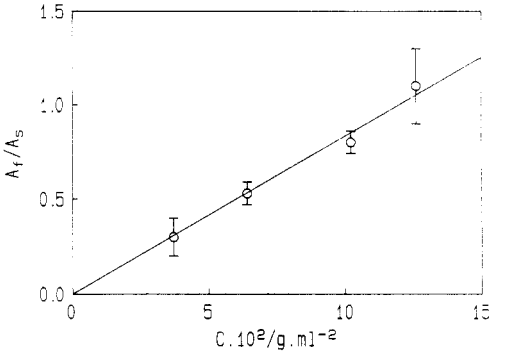

Figure 11. Plot of the averaged values of A_f/A_s versus the polymer concentration. System as in Figure 10.

ation time obtained from DLS experiments is given by eq 13. Thus the molecular weight dependence is the same in both cases but the concentration dependence is expected to be stronger in the case of DLS. Values of $T_r(D_g/D_h)$ from the experimental data of Adam and Delsanti for T_r are indicated in Figure 8. The approximate agreement suggests a close relationship between the slow relaxation times observed in DLS and the relaxation times observed in mechanical measurements.

Adam and Delsanti performed DLS experiments similar to those reported here.[9] Lacking a multi-τ correlator, they measured the correlation curve at different time windows. They analyzed the data by force fitting to a single-exponential function and obtained a relaxation rate that depended on the time window. At short times a q^2-dependent relaxation time was found which agrees well with our data (see Figure 9). At long times a q-independent relaxation time was found, which they compared directly with the slowest relaxation time from viscosity measurements instead of via eq 13, without giving a theoretical justification for this direct comparison. However, D_g/D_h is not very different from unity for the concentration range investigated, which makes it difficult to check experimentally the validity of this term. They found a very close agreement between these two experiments, but as our experiments show (especially for the higher concentrations) since there is no clearly distinct slowest relaxation time, a quantitative comparison in this way is in our opinion not meaningful.

From the theory described above, it is expected that the ratio of the amplitude of the fast mode to that of the slow mode will be independent of the wave vector and increase linearly with polymer concentration (see eq 14). The dependence of A_f/A_s on the wave vector is shown in Figure 10. Here we have taken for A_s the sum total of all the modes slower than the diffusive mode. Although the data scatter, there does not seem to be a systematic dependence on q. The average ratio increases linearly with the polymer concentration as $A_f/A_s = 8.3C$ (see Figure 11). Using eq 8 and 10 in eq 14 we may write $A_f/A_s = \xi_h^{-1}(a/f)$. If we use for ξ_h the experimental value given above, we have an alternative way of calculating f yielding $f = 4.1 \times 10^{-2}$. This value is somewhat larger than the value of f obtained from the cooperative diffusion coefficient but is possibly within the experimental error in view of the use of only a limited number of values of A_f/A_s and the relatively large uncertainty in these values.

As mentioned above, the sample with $M_w = 1.28 \times 10^6$ shows a qualitatively different behavior at small scattering vectors. In Figure 12 relaxation time distributions are shown for different values of q^2. The slowest and fastest relaxation rates are plotted as a function of q^2 in Figure 13. For large scattering vectors the behavior is analogous to that in the other semidilute solutions, i.e., a q^2-dependent fast mode and a number of q-independent slower modes. At small scattering vectors, however, the correlation function is apparently dominated by a single-exponential decay rate, which increases over the very limited range of accessible q values. This behavior can be explained in terms of the theory discussed above. For large scattering vectors, where $D_e q^2 > T_r^{-1}$, we are in the gel regime. For small scattering vectors, where $D_e q^2 < T_r^{-1}$, we are in the hyrodynamic regime. This means that D_e is equal to D_g at high values of q and D_h at low values of q. The diffusion coefficient found at

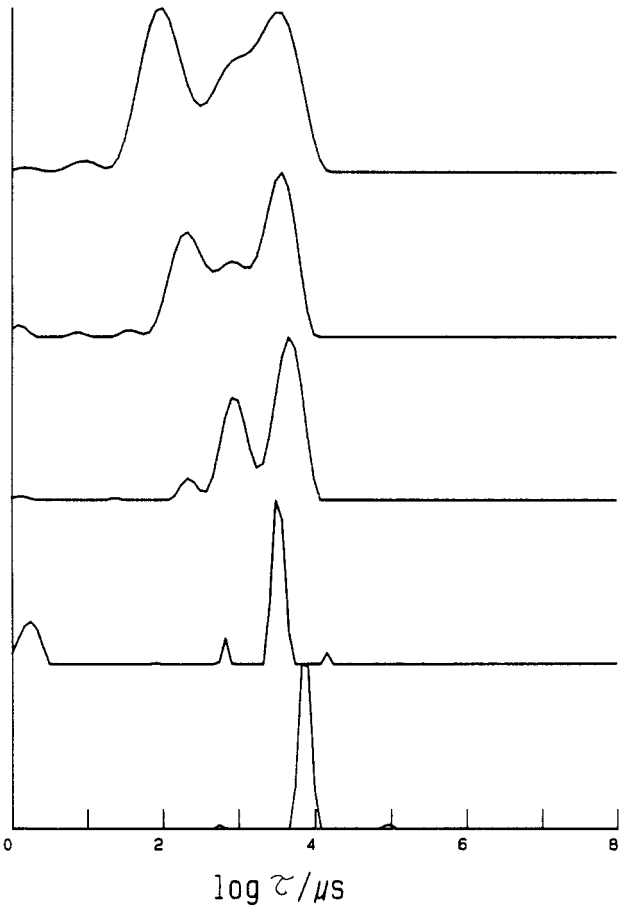

Figure 12. Relaxation time distributions obtained from REPES for a semidilute solution of polystyrene in cyclohexane at 35 °C ($M_w = 1.28 \times 10^6$, $C = 6.6 \times 10^{-2}$ g mL^{-1}) for different scattering vectors. From bottom to top $q^2 = 0.24 \times 10^{14}$, 0.53×10^{14}, 2.0×10^{14}, 4.0×10^{14}, and 11.8×10^{14} m^{-2}.

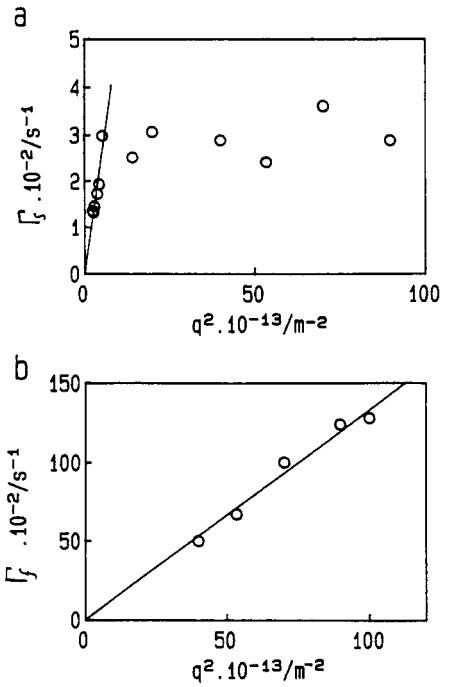

Figure 13. Plot of the decay rates of the slowest (a) and the fastest (b) mode versus q^2 for a semidilute solution of polystyrene in cyclohexane at 35 °C. The decay rates of the single mode at very small scattering vectors are included in part a. System as in Figure 12.

large scattering vectors fits the values found for other semidilute solutions (see Table I), which means that we are measuring D_g. The value $D_e = 5 \times 10^{-12}$ m^2/s obtained from a limited range of small scattering vectors is closer to the value of $D_h = 8.4 \times 10^{-12}$ m^2/s interpolated from classical gradient experiments, although somewhat smaller.

Intermediate Concentrations. As discussed above, up to a concentration of $\sim 5 \times 10^{-3}$ g/mL one observes a diffusional mode representing the self-diffusion of the coils and, at higher scattering angles, additional faster modes due to internal motions of the individual coils. For concentrations larger than $\sim 3 \times 10^{-2}$ g/mL one again observes a single diffusional mode representing in this case the cooperative diffusion of the transient gel and, in addition, a number of slower modes. In the concentration range between $\sim 5 \times 10^{-3}$ and $\sim 3 \times 10^{-2}$ g/mL the relaxation time distribution smoothly crosses over between these two situations as is shown for one scattering vector in Figure 14. The slowest mode changes progressively from a q^2 dependent mode at the lowest concentration to a q independent mode at the highest concentration. The relative contribution of faster modes increases with increasing concentration and these appear also at lower values of q. These faster modes cannot be attributed to internal motions of the individual coils, as the influence of these motions to the correlation function is negligible if $qR_g < 1$. One way of explaining these modes would be that they result from a coupling of internal modes over distances larger than R_g of chains that begin to interpenetrate at these concentrations, resulting at high concentrations in elastic interactions of the whole transient network. At these higher concentrations the diffusion of the individual coils becomes very slow and no longer contributes to the correlation function if the solution becomes homogeneous over distance scales larger than R_g. For these concentrations the autocorrelation function is determined by the cooperative diffusion coefficient and the viscoelastic properties of the transient gel.

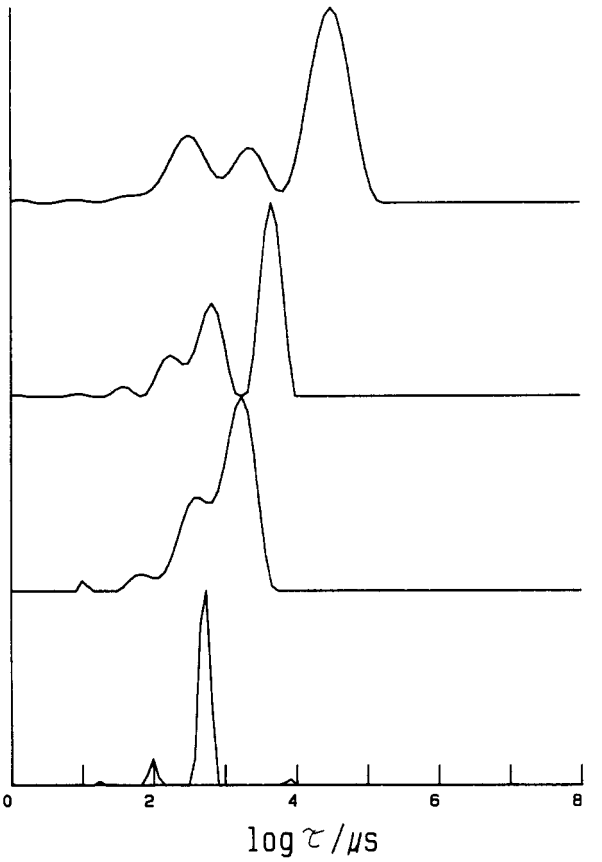

Figure 14. Relaxation time distributions obtained from REPES of intermediate concentrations of polystyrene in cyclohexane at 35 °C at a fixed molecular weight and scattering vector ($M_w = 3.8 \times 10^6$, $q^2 = 4.0 \times 10^{14}$ m^{-2}): C is 0.5×10^{-2}, 1.0×10^{-2}, 1.4×10^{-2}, and 2.8×10^{-2} g mL^{-1} (bottom to top).

Conclusion

From the foregoing discussion we may conclude the following:

(1) The autocorrelation curves obtained from DLS on semidilute solutions of high molecular weight linear polystyrene in Θ solvents are much more complicated than was concluded from earlier experiments. The autocorrelation of the scattered light can be modeled as a multiexponential function with decay times over a wide range on the time scale. Using a double-exponential function to describe $g_{(1)}(t)$ is a gross approximation of the true autocorrelation function.

(2) The relaxation time distributions obtained from the Laplace transformation of $g_{(1)}(t)$ measured in the semidilute concentration regime show a fast diffusive mode, which becomes increasingly important at higher concentrations, and a number of approximately q-independent slower modes.[40]

(3) The diffusion coefficient obtained from the fast mode represents the cooperative diffusion of the transient network. Its concentration behavior can be quantitatively explained when we take into account both the ternary excluded-volume interactions and the elastic forces due to topological entanglements. As these two types of interactions have different concentration dependencies, their relative contributions to the autocorrelation function change with changing concentration.

(4) The broad range of slow relaxation times is probably related to the viscoelastic properties of the transient network. For a more detailed appraisal of the slow modes it is necessary to make parallel mechanical measurements on the same solution as the DLS measurements

and analyze the data in a similar way in order examine the relationship between the respective relaxation time distributions. Such studies have been initiated.

Measurements of the relaxation time distributions as a function of solvent quality show that the relative amplitudes of the slow modes decrease with increasing solvent quality and thus increasing thermodynamic interactions, but they remain observable even for good solvents.

References and Notes

(1) de Gennes, P.-G. *Macromolecules* **1976**, *9*, 587, 594.
(2) de Gennes, P.-G. *Scaling Concepts in Polymer Physics*; Cornell University Press: London, 1979.
(3) Doi, M.; Edwards, S. F. *The Theory of Polymer Dynamics*; Oxford University Press: Oxford, 1986.
(4) Stepanek, P.; Konak, C. *Adv. Colloid Interface Sci.* **1984**, *21*, 195.
(5) Chu, B.; Nose, T. *Macromolecules* **1979**, *12*, 590, 599.
(6) Amis, E. J.; Han, C. C.; Matsushita, Y. *Polymer* **1984**, *25*, 650.
(7) Takahashi, M.; Nose, T. *Polymer* **1986**, *27*, 1071.
(8) Adam, M.; Delsanti, M. *J. Phys. (Paris) Lett.* **1984**, *45*, L-279.
(9) Adam, M.; Delsanti, M. *Macromolecules* **1985**, *18*, 1760.
(10) Brown, W. *Macromolecules* **1986**, *19*, 387, 1083.
(11) Brown, W.; Johnsen, R. M. *Macromolecules* **1986**, *19*, 2002.
(12) Brown, W.; Stepanek, P. *Macromolecules* **1988**, *21*, 1791.
(13) Brown, W.; Johnsen, R. M.; Stepanek, P.; Jakes, J. *Macromolecules* **1988**, *21*, 2859.
(14) Stepanek, P.; Konak, C.; Jakes, J. *Polym. Bull.* **1986**, *16*, 67.
(15) Stepanek, P.; Jakes, J.; Hrouz, J.; Brown, W. In *Polymer Motion in Dense Systems*; Richter, D., Springer, T., Eds.; Springer Proceedings in Physics, 1988; Vol. 198, p 29.
(16) Brochard, F.; de Gennes, P.-G. *Macromolecules* **1977**, *10*, 1157.
(17) Brochard, F. *J. Phys. (Paris)* **1983**, *44*, 39.
(18) Rouse, P. E. *J. Chem. Phys.* **1953**, *21*, 1272.
(19) Zimm, B. H. *J. Chem. Phys.* **1956**, *24*, 269.
(20) Pecora, R. *J. Chem. Phys.* **1965**, *43*, 1562.
(21) Yamakawa, H. *Modern Theory of Polymer Solutions*; Harper&Row: New York, 1974.
(22) Jakes, J., unpublished results.
(23) Provencher, S. W. *Makromol. Chem.* **1979**, *180*, 247.
(24) Livesey, A. K.; Delaye, M.; Licinio, P.; Brochon, J. E. *Faraday Discuss. Chem. Soc.* **1987**, *83*, 247.
(25) Livesey, A. K.; Delaye, M.; Licinio, P. *J. Chem. Phys.* **1986**, *84*, 5102.
(26) Jakes, J. *Czech. J. Phys. B* **1988**.
(27) Nicolai, T.; Brown, W.; Johnsen, R. M. *Macromolecules* **1989**, *22*, 2795. press.
(28) Geisler, E.; Hecht, A. M. *J. Phys. Lett.* **1979**, *40*, L-173.
(29) Ferry, J. D. *Viscoelastic Properties of Polymers*, 3rd ed.; Wiley: New York, 1980.
(30) Roots, J.,; Nyström, B. *Macromolecules* **1980**, *13*, 1595.
(31) Raju, V. R.; Menezes, E. V.; Marin, G.; Graessley, W. W., Fetters, L. J. *Macromolecules* **1981**, *14*, 1668.
(32) Wang, C. H.; Fisher, E. W. *J. Chem. Phys.* **1985**, *82*, 632.
(33) Wang, C. H.; Fisher, E. W. *J. Chem. Phys.* **1985**, *82*, 4332.
(34) Adam, M.; Delsanti, M. *J. Phys. (Les Ulis, Fr.)* **1983**, *44*, 1185.
(35) Adam, M.; Delsanti, M. *J. Phys. (Les Ulis, Fr.)* **1984**, *45*, 1513.
(36) Osaki, K.; Nishizawa, K.; Kurata, K. *Macromolecules* **1982**, *15*, 1068.
(37) Takahashi, Y.; Noda, I.; Nagasawa, M. *Macromolecules* **1985**, *18*, 2220.
(38) Takahashi, Y.; Umeda, M.; Noda, I. *Macromolecules* **1988**, *21*, 2257.
(39) *Base line* taken to equal the total number of counts times the number of counts per second.
(40) **Note Added in Proof**. It cannot be ruled out, however, that the split-up of the slow part of the decay time distribution is not artifactual and derives from modulation of the experimental correlogram by a small amount of systematic noise. A subsequent communication will deal with application of the generalized exponential distribution (GEX) to describe the total of all the slow components as an alternative procedure.

Registry No. Polystyrene, 9003-53-6.

Local Orientational Motions in Flexible Polymeric Chains

Ivet Bahar* and Burak Erman

Polymer Research Center and School of Engineering, Bogazici University, Bebek 80815, Istanbul, Turkey

Lucien Monnerie

Laboratoire de Physico-Chimie Structurale et Macromoléculaire, associé au C.N.R.S., 10, rue Vauquelin, 75 231 Paris Cedex 05, France.

Received March 24, 1989; Revised Manuscript Received July 26, 1989

ABSTRACT: Effects of chain connectivity, viscous resistance of the environment, and internal barriers to conformational transitions are studied in relation to local orientational motions in flexible chains. Calculations are performed according to the dynamic rotational isomeric states scheme. Only a single transition over a bond at a time is assumed. That such single bond rotations are indeed possible in a sequence of 20 bonds without significant distortion of the tails is shown by the present analysis. The increase in the frictional resistance to motion with the size of the mobile sequence is investigated for polyethylene at 300 K. The latter, referred to as the size effect, is included in the treatment through consideration of the total path traveled by each of the moving atoms. Orientational autocorrelation functions for a bond at the end of an N bond mobile sequence are evaluated in the presence and absence of the size effect. Two different correlation times, emphasizing short and long time motions, are defined. Dependence of the correlation times on the length of the mobile sequence is evaluated.

Introduction

Long- and short-wavelength motions in a single polymer chain are controlled by three major factors: (i) the external resistance to motion exerted by the environmental frictional forces; (ii) the internal resistance associated with barriers to conformational transitions; (iii) the chain connectivity.

The first two factors are common to both small molecules and macromolecules. The third is an inherent property of macromolecules uniquely and distinguishes them

0024-9297/90/2223-1174$02.50/0